Electrochemistry Communications 12 (2010) 496–498

Contents lists available at ScienceDirect

Electrochemistry Communications

journal homepage: www.elsevier.com/locate/elecom

An understanding of anomalous capacity of nano-sized CoO anode materials for advanced Li-ion battery

C.H. Chen [a], B.J. Hwang [a,b,*], J.S. Do [c,d], J.H. Weng [d], M. Venkateswarlu [a], M.Y. Cheng [a], R. Santhanam [e], K. Ragavendran [a], J.F. Lee [b], J.M. Chen [b], D.G. Liu [b]

[a] Nano-Electrochemistry Lab., Department of Chemical Engineering, National Taiwan University of Science and Technology, #43 Keelung Rd., Sec. 4, Taipei 106, Taiwan
[b] National Synchrotron Radiation Research Center (NSRRC), Hsinchu, Taiwan
[c] Department of Chemical and Materials Engineering, National Chin-Yi University of Technology, Taichung 411, Taiwan
[d] Department of Chemical and Materials Engineering, Tunghai University, Taichung 407, Taiwan
[e] Solid State and Surface Sciences Lab., Department of Physics, Southern University, Baton Rouge, LA-70808, USA

ARTICLE INFO

Article history:
Received 13 November 2009
Received in revised form 21 January 2010
Accepted 21 January 2010
Available online 28 January 2010

Keywords:
CoO
EXAFS
Lithium batteries
Anode
Anomalous capacity

ABSTRACT

Nanostructured transition metal oxides are of great interest as a new generation of anode materials for high energy density lithium-ion batteries. In this work, research has been focused on the nano-sized (grain size ~7 nm) CoO anode material and this material delivers charge capacity of 900 mAh g^{-1} that exceeds the theoretical value of 715 mAh g^{-1}. Possible reason for this unaccounted and unexplained anomalous capacity of the nano-sized CoO material has been suggested by thermogravimetric analysis. A mechanism for this interesting behavior has been systematically evaluated by using X-ray absorption spectroscopy. The anomalous capacity is proposed to be associated with the formation of oxygen-rich CoO material. The results obtained from the nano-sized CoO material have been compared with relatively larger-sized material (grain size ~32 nm).

1. Introduction

Transition metal oxides (TMOs) have been widely investigated as promising anode materials for lithium-ion batteries since the discovery of Tarascon and co-workers [1]. They demonstrated that the electrodes made of TMO nanoparticles could deliver excellent electrochemical performance, particularly Co-based oxides. The mechanism of Li storage with these transition metal oxides differs from the classical Li insertion/deinsertion in graphite anodes or Li-alloying processes in alloy electrodes. The mechanism involves the formation and decomposition of Li_2O, (for example, $CoO + 2Li^+ + 2e \rightarrow Co + Li_2O$), accompanied by the reduction and oxidation of metal nanoparticles, respectively. Reactions of this type involve two electrons and hence deliver a higher capacity compared to conventional graphite anodes. Higher capacity can be expected for such reactions if the metal components are further lithiated by alloying reaction with lithium [2]. Also, the formation and decomposition reactions are known for their notable SEI layer formations at low potentials [3,4], which results in capacity rise. However, these reactions suffer from poor energetic yield owing to large hysteresis in the charge–discharge curves [5]. Interestingly, it has been reported that this hysteresis decreases as the electro-negativity of the anion decreases, with the lowest values for transition metal phosphides. In the present communication, to our knowledge for the first time, we demonstrate an interesting observation of anomalously high capacity of nano-sized CoO electrode during lithium insertion/deinsertion reactions.

2. Experimental

$Co(OH)_2$ was prepared by mixing 100 ml of 1.0 M cobalt nitrate solution (J.T. Baker, $Co(NO_3)_2{\cdot}6H_2O$, >99.1%) and 500 ml of 0.4 M sodium hydroxide solution (Merck, NaOH, >99%) in a flask and stirring for 8 h under nitrogen atmosphere. The obtaining $Co(OH)_2$ was washed and dried in a vacuum oven at 50 °C for 24 h. Subsequently cobalt oxides were obtained by heating $Co(OH)_2$ at 200 (CoO-A) and 900 °C (CoO-B), respectively, for 12 h in N_2. X-ray diffraction analysis was conducted using Cu-Kα (λ = 1.5418 Å) radiation in 2θ range between 10° and 80°, at a scan rate of 5° min^{-1}. All the diffraction patterns were identified to be cubic rock salt structure (JCPDS 78-0431). The average grain size was calculated using the Scherrer's formula and the surface area was measured using the BET surface area analyzer. Thermogravimetric analysis was

* Corresponding author. Address: Nano-Electrochemistry Lab., Department of Chemical Engineering, National Taiwan University of Science and Technology, # 43 Keelung Rd., Sec. 4, Taipei 106, Taiwan. Tel.: +886 2 27376624; fax: +886 2 27376644.
E-mail addresses: bjh@mail.ntust.edu.tw, bjh@ch.ntust.edu.tw (B.J. Hwang).

1388-2481/$ - see front matter © 2010 Published by Elsevier B.V.
doi:10.1016/j.elecom.2010.01.031

performed between 30 and 900 °C at a rate of 5 °C min^{-1} in flowing nitrogen to determine the oxygen content. The electrochemical measurements were performed using coin-type cells with lithium as anode. Working electrode was composed of CoO active material, carbon black and polyvinylidene fluoride (PVdF) in a weight ratio of 3:1:1 in *N*-methyl-2-pyrrolidinone (NMP). A polypropylene film (Ashahi N910) was used as the separator and the electrolyte was 1.0 M $LiPF_6$ in a 1:1 mixture of ethylene carbonate and diethyl carbonate. The cell was assembled in an argon filled glove box with both moisture and oxygen level below 2 ppm. Galvanostatic charge/discharge cycle was performed using Maccor battery tester. X-ray absorption spectroscopy (XAS) experiments were carried out on the Co and O K-edges at beam line BL-17C in a storage ring of 1.5 GeV at National Synchrotron Radiation Research Center (NSRRC), Hsinchu, Taiwan. The measurements were carried out using Si (1 1 1) double crystal monochromator. Detailed XAS experimental procedure can be found from our previous report [6].

3. Results and discussion

Fig. 1 shows the typical XRD patterns of the different CoO samples, CoO-A and CoO-B, prepared at different calcination temperatures, 200 °C and 900 °C, respectively, in nitrogen atmosphere. All the peaks of the two patterns are well indexed as cubic CoO phase with rock salt structure (JCPDS file No. 78-0431) and with a space group of *Fm3m*. However, the intensity of CoO-B is much stronger than that of CoO-A, indicating the nanocrystalline nature of CoO-A. In our previous study, we found that an increase in the oxidation state of the Co leads to amorphous characteristic in the XRD [7]. This indicates a possible higher oxidation state of CoO-A. The average grain size of CoO-A and CoO-B samples was calculated as 6.59 and 31.5 nm, respectively. The BET surface area of CoO-A and CoO-B, respectively, was determined as 89.82 and 0.47 $m^2\ g^{-1}$.

The initial charge/discharge profiles of CoO-A and CoO-B, recorded at a rate of 0.1 C (71.5 mAh g^{-1}, theoretical capacity of CoO = 715 mAh g^{-1}) between 0.02 and 3.0 V are shown in Fig. 2. The theoretical capacity of CoO used in this work, was based on the following conversion reaction

$$CoO + 2Li^+ + 2e^- \rightarrow Li_2O + Co \quad (1)$$

Three distinct plateaus are clearly seen in the discharge profiles (Li insertion) of both CoO-A and CoO-B. The first plateau appearing at 1.2 V (40 mAh g^{-1}) and 0.8 V (25 mAh g^{-1}) for CoO-A and CoO-B, respectively, is associated with the lithium storage into CoO. The second flat plateau located at 1.0 V (820 mAh g^{-1}) and 0.85 V (490 mAh g^{-1}) for CoO-A and CoO-B, respectively, can be ascribed to the conversion reaction between CoO and Li (Eq. (1)). The third plateau (declined line), below 0.5 V, accounts for 414 mAh g^{-1} for CoO-A and 360 mAh g^{-1} for CoO-B, could be attributed to the interaction of nano-sized Co particle with the electrolyte for the formation of solid electrolyte interface (SEI) layer. The charge profiles (Li deinsertion) of CoO-A and CoO-B consist of two regions. The first region located between 0.0 and 1.8 V, accounts for the capacity

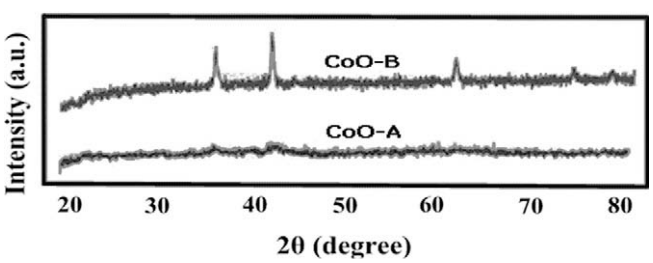

Fig. 1. XRD patterns of CoO-A and CoO-B.

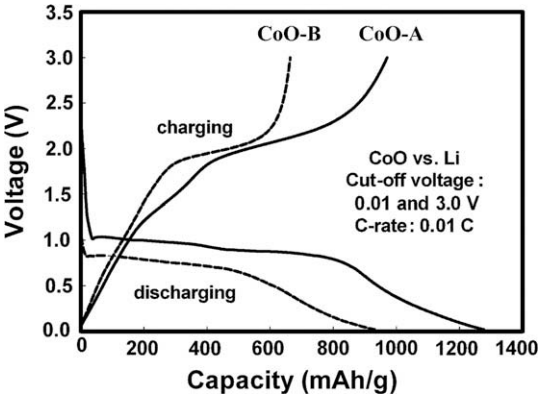

Fig. 2. Charge–discharge curves of CoO-A and CoO-B.

of 400 mAh g^{-1} for CoO-A and 300 mAh g^{-1} for CoO-B, is associated with the interactions between nano-sized Co and the electrolyte. The second flat plateau appeared close to 2.0 V, can be attributed to the oxidation of nano-sized Co particles with Li_2O. In this region, CoO-A and CoO-B delivered the capacity of 500 mAh g^{-1} and 200 mAh g^{-1}, respectively. Overall, CoO-A and CoO-B delivered initial discharge capacities of 1274 and 831 mAh g^{-1}, and charge capacities of 900 and 500 mAh g^{-1}, respectively. It is immediately apparent that the charge capacity values for CoO-A are significantly greater than the theoretically expected capacities for CoO. Note that the CoO-A show an initial coulombic efficiency of approximately 71% which is notably higher than that of CoO-B (60%). The origin of higher capacity and enhanced electrochemical behavior of CoO-A should essentially be attributed to the smaller size with larger surface area than CoO-B. Therefore, CoO-A could provide more reaction sites on the surface and the smaller diameter provides a short diffusion length for Li diffusion, which could enhance the charge transfer and the electrochemical reactions [8].

Since the capacity obtained for CoO-A sample is 20% higher than expected theoretical capacity, we hypothesize that the amount of anomalous capacity could be related to the participation of excess oxygen in the electrochemical behavior of nano-sized CoO sample. To check our hypothesis, thermogravimetric (TGA) measurements were carried out on CoO-A and CoO-B samples (Fig. 3). In Fig. 3,

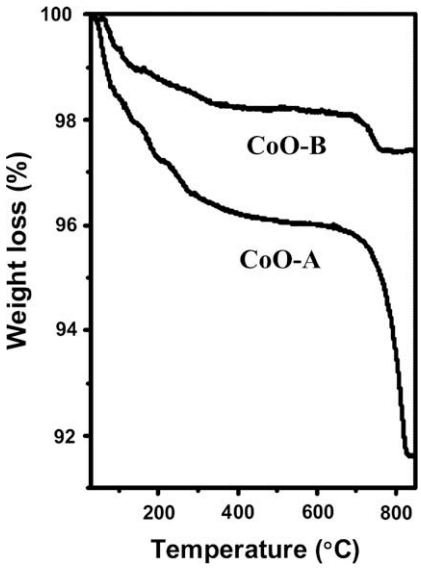

Fig. 3. TGA curves of CoO-A and CoO-B.

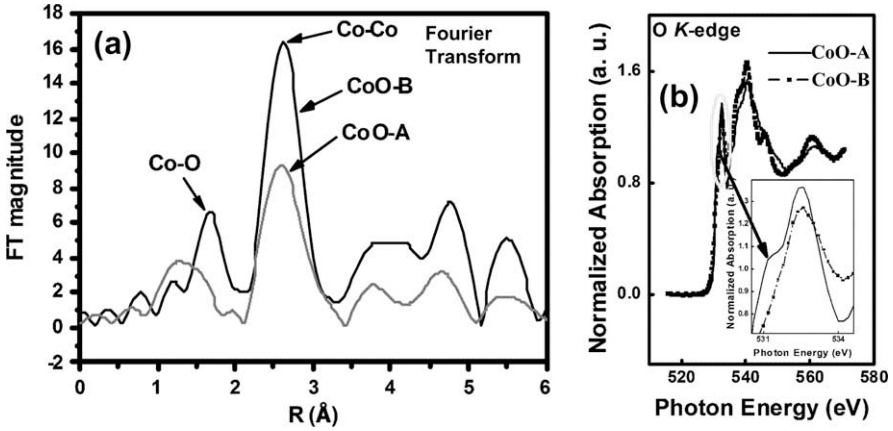

Fig. 4. (a) FT-EXAFS at Co K-edge and (b) XAS spectra at oxygen K-edge of CoO-A and CoO-B.

the first weight loss at <300 °C, and the second weight loss between 695 and 826 °C are due to dehydration and decomposition of excess oxygen on CoO surface, respectively. However the TGA for micron-sized commercial $Co(OH)_2$ (not shown) only exhibits weight loss at the temperature range less than 300 °C, indicating the surface oxygen for micron-sized $Co(OH)_2$ is hardly detected. From the amount of weight loss, the excess oxygen contents were calculated as 0.157 mol and 0.029 mol, respectively, for CoO-A and CoO-B samples. Hence, Eq. (1) can be reasonably modified as

$$CoO_{(1+\delta)} + (2+\delta)Li^+ + 2e^- \rightarrow (1+\delta)Li_2O + Co \quad (2)$$

Synchrotron radiation-based X-ray absorption spectroscopy (XAS) measurements were carried out to further understand and confirm the active participation of oxygen for the anomalous or surplus capacity delivered by nano-sized CoO samples. XAS measurement has great potential to examine the electronic and local structure of a specific atom in the electrode materials for use in lithium-ion batteries [9,10]. Fig. 4a shows the Fourier transforms of the extended X-ray absorption fine structure (FT-EXAFS) at Co K-edge for both CoO-A and CoO-B samples. The peak at ~1.45 Å for CoO-A and at ~1.6 Å for CoO-B can be attributed to the Co–O bond in the first coordination shell of Co. The second peak at ~2.5 Å for both samples corresponds to the Co–Co bond, which is due to the contribution of 12 coordinated Co atoms in the edge shared CoO_6 octahedra. Further, the peaks around 3.9, 4.8 and 5.6 Å can be ascribed to the double scattering of Co–O–Co at the corner shared octahedra, the single scattering path of Co–Co and the double scattering of Co–Co–Co, respectively [8]. The EXAFS data fitting results exhibit a significantly smaller Co–O bond distance for CoO-A than that of CoO-B while the rest of the bond distances are almost identical. In addition, the ratio of Co–O to Co–Co coordination number (CN) for CoO-A (5.0–8.8) and CoO-B (5.4–11.6) is different. Thus, the oxygen-to-cobalt ratio can be calculated and it has been found to be 1.12 and 1.02 for CoO-A and CoO-B, respectively. This result indicates 0.12 mol excess oxygen which corresponds to 85.8 mAh g^{-1}, slightly lower than the observed capacity (105 mAh g^{-1}) in the discharge plateau at 1.0 V for CoO-A. The discrepancy may be resulted from the limitation of the structural model to determine the CN. The X-ray Absorption Near-Edge Structure (XANES) of CoO-A and CoO-B at O K-edge is measured in the fluorescence mode and is shown in Fig. 4b. Small peaks appearing at 527.4 and 528.2 eV in the pre-edge region can be ascribed to the electronic transition from 1s to 2p orbital. It is noted that the peak intensity of CoO-A is slightly higher than that of CoO-B, indicating higher possibility of electronic transition for CoO-A from 1s to 2p oxygen and/or Co 4sp hybridized orbital. It also implies less Co–O ratio for CoO-A. In addition, the XANES at Co K-edge (not shown) indicates the averaged valence state of Co is higher for CoO-A than for CoO-B, implying the surface Co possesses higher valence state for CoO-A. The XANES results are in good agreement with the TGA, EXAFS and electrochemical analysis.

4. Conclusions

In this study, the anomalously high capacity has been investigated in nano-sized CoO anode material. XAS investigations suggests (i) a higher averaged oxidation state of Co atom in CoO-A sample due to its nano-sized nature, and (ii) excess oxygen content in CoO-A sample in consistent with TGA analysis. From the above results, it is reasonable to believe that the excess oxygen plays a pivotal role in the origin of the anomalously high capacity. The surplus capacity beyond the amount of expected theoretical capacity can possibly be exploited to develop future lithium-ion batteries with significantly higher energy density than the current state-of-the-art batteries.

Acknowledgements

We acknowledge the financial support from the National Science Council (NSC) under a special program on Nanoscience and Nanotechnology (NSC-97-2120-M-011-001), Distinguished Scholars Research Project (NSC-97-2221-E-011-075-MY3), and Energy Technology Program (NSC-98-ET-E-011-003-ET) and support from National Synchrotron Radiation Research Center (NSRRC) and National Taiwan University of Science and Technology (NTUST).

References

[1] P. Poizot, S. Larulle, S. Grugeon, L. Dupont, J.M. Tarascon, Nature 407 (2000) 496.
[2] C.H. Kim, Y.S. Jung, K.T. Lee, J.H. Ku, S.M. Oh, Electrochim. Acta 54 (2009) 4371.
[3] J.T. Li, V. Maurice, J. Swiatowska-Mrowiecka, A. Seyeux, S. Zanna, L. Klein, S.-G. Sun, P. Marcus, Electrochim. Acta 54 (2009) 3700.
[4] C. Chen, N. Ding, L. Wang, Y. Yu, I. Lieberwirth, J. Power Sources 189 (2009) 552.
[5] F. Gillot, M. Ménétrier, E. Bekaert, L. Dupont, M. Morcrette, L. Monconduit, J.M. Tarascon, J. Power Sources 172 (2007) 877.
[6] B.J. Hwang, Y.W. Tsai, R. Santhanam, D.G. Liu, J.F. Lee, J. Electrochem. Soc. 150 (2003) A335.
[7] J.S. Do, C.H. Weng, J. Power Sources 146 (2006) 482.
[8] B.J. Hwang, Y.W. Tsai, C.H. Chen, R. Santhanam, J. Mater. Chem. 13 (2003) 1962.
[9] B.D. Cullity, Elements of X-Ray Diffraction, Addison-Wesley, 1956.
[10] C.H. Choi, S.Y. Lee, S.B. Kim, M.G. Kim, M.K. Lee, H.J. Shin, J.S. Lee, J. Phys. Chem. B 106 (2002) 9252.